

**OPTIMIZING THE LASER PARAMETERS TO ATTAIN THE MAXIMUM
HARDNESS IN COBALT BASED (STELLITE - 6) HARDFACED SURFACES**

A. Umesh Bala*, Dr.R. Varahamoorthi

**Research Scholar, Department of Manufacturing Engineering, Annamalai University, Tamil Nadu, India.
Associate Professor, Department of Manufacturing Engineering, Annamalai University, Tamil Nadu, India.*

ABSTRACT: Laser Hardfacing are naited mainly to improve the service life of engineering components either rebuilding or fabricating in such a way to produce a composite wall section to wear, erosion, corrosion, etc. The main characteristics of CO₂ laser hardfaced surfaces are good metallurgical bonding, low heat input and less dilution. In this paper, a provare has been made to optimize the process parameters of laser hardfaced surfaces such as Laser Power(P), Travel Speed(T), Defocusing Distance(D) and Powder feed rate(F).The optimization of laser hardfaced surfaces have good product development, value annexation, revive and restoration. The laser hardfacing is carried out by CO₂laser by coaxial - powder feeding method. Inthis hardfacing process AISI 304 stainless steel is used as the base metal and the cobalt basedStellite 6 powder is used as hardfaced material. The influence of theprocessing variables on hardness is bespeaked for optimized condition. The experiments were conducted based ona four factor and five level central composite rotatable design. The mathematical model wasdeveloped using Response Surface Methodology(RSM) technique to predict the hardness. The interaction effects of input processparameters of laser hardfacing were discussed. The optimized process parameter for laser hardfacing and the influenced parameterwere identified.

Key words: Optimization, RSM, Stellite-6, Laser Hardfacing, AISI 304 SS.

I. INTRODUCTION

Industrial applications exiger parts of components with explicit surface properties such as good wear resistance, corrosion resistance and toimprove the mechanical properties especially hardness. Alloys with those properties are usually very expensive and there is a great interest in reducing the cost of components for gratifying these requirements. In this perceide, laser hardfacing has been used as a cost-effective technique to improve the surface properties of materials by use of the laser beam heat for modification of its structure and physical characteristics. Laser hardfacing results inincreasing the hardness, toughness and wear resistance of the material surface in a very short time. CO₂, Nd: YAG and diode lasers have been the most commonly used types. The surface properties can also be improved by deposit a protective layer. This type of protective layers can also be produced with the Laser hardfacing process in which the thickness can produce in the range of 0.3-2 mm thick coating onto a work piece, joining both materials by a fusion bond. A hardfaced track is obtained by injecting powder particles into the molten pool produced by a moving laser beam.StainlessSteels contain both chromium and nickel. AISI 304Stainless steels are the most wear resistant, ductile, and weldable type of steel. The base material 304 stainless steels areubiquitously used in industries due to its thermal conductivity, high stability at elevatedtemperatures and superior absorption of laser energy. Stellite-6 is a useful hardfacing alloy in which chromium provides corrosion and wear resistance while carbides add strength to the alloy. Molybdenum(Mo) and tungsten (W) are solid solution hardening elements andalso contribute to the strength of Stellite-6 through precipitation hardening by formation of carbides and intermetallic phases such as Co, Mo and W. There are recent studies performed on Stellite hardfacing using various methods such as Tungsten Inert Gas hardfacing, PlasmaTransfer Arc hardfacing and laser hardfacing. Among these laser hardfacingproduced on stainless steel indicate better performance than other techniques. Hardfacing carriedout by the laser using Stellite-6 has been focused on important aspects such as evolution of hardness, wear resistance of hardfaced surface and the effects of laser processing parameters on the hardfacing geometry, fissure and on microstructure.

Table 1: Chemical composition (wt.%) of base material (AISI 304).

C	Mn	Ni	Si	P	S	Cr	Fe
≤ 0.12	≤ 2.0	8.00–11.00	≤ 1.0	≤ 0.035	≤ 0.03	17.00–19.00	Balance

In laser hardfacing, temperature gradients on the melt surface between the laser-beam impact point and the intersection line of the solid-liquid interface, these surface generate the surface-tension gradients that sweep liquid away from beam impact point. The resulting flow of liquid creates a depression of the liquid surface beneath the beam and ridging of the liquid surface. As the beam passes to other areas of the surface, this distortion of the liquid surface is frozen, creating a roughened rippled surface. This type of hardfacing may be applied to a new part during production to increase its wear resistance, or it may be used to restore a worn-out surface. Regardless of low efficiency, CO₂ lasers have a better beam quality and focusability than other types of lasers with the same power. CO₂ lasers also have the advantages of being very well absorbed by organics, glass and ceramic materials and are relatively color independent. As a result, selecting a CO₂ laser is a trade-off between economical issues and the performance of the laser in different industrial applications. Although the high maintenance cost and low wall plug efficiency are two restrictions for applications of CO₂ lasers, this laser has been widely adopted for usage in industrial applications such as welding, cutting, hardfacing, and processing of glass, ceramics, and organic (e.g., polymer textile, paper, tissue material, and food) materials. Hardfacing can also be done by other welding techniques like as SMAW, GMAW, SAW, ESW, PTAW. Among these laser is one of the highest power density sources recently available in Industries for hardfacing of materials.

Table 2: Chemical composition (wt%) of Powder material (Stellite-6).

Cr	C	W	Mo	Ni	Si	Fe	Mn	S	Co
28.5	1.12	5.06	0.35	1.34	1.13	0.99	0.4	0.01	Balance

II. EXPERIMENTAL WORK

2.1 IDENTIFY THE IMPORTANT PROCESS VARIABLES AND ITS LIMITS:

Laser hardfacing experimental runs were executed based on trials. The Base material 304 stainless-steel plate of 14 mm-thick and cobalt based (Stellite-6) hardfacing powder material were used to find out the feasible working limits of laser hardfacing parameters. The trial experiments were conducted and the working range was decided based on the quality appearance and the absence of any visible defects. Different combinations of parameters were used to carry out the trial experiments. This was done by varying any one of the factor from minimum to maximum while keeping the other parameters at constant. The working limits of the individual parameters were identified by macrostructure. Laser hardfaced deposit which was exposed to a smooth appearance without any visible macro level defects such as crack, pores were chosen as the feasible working limits. The identified input parameters are: Laser Power (P), Travel Speed (T), Defocusing Distance (D) and Powder Feed Rate (F). The upper limit was coded as + 2 whereas the lower limit -2 by using the input parameters and their working range the design matrix was developed and the experiments were conducted as per the design matrix. The laser hardfacing parameters and their limits are tabulated in Table:3

Table 3: Laser hardfacing parameters and their limits.

Parameters	Units	Notations	Levels				
			-2	-1	0	1	2
Laser Power	W	P	2200	2400	2600	2800	3000
Travel Speed	mm/min	T	400	500	600	700	800
Defocusing Distance	mm	D	16	18	20	22	24
Powder Feed Rate	g/min	F	4	8	12	16	20

2.2 EXPERIMENTAL DESIGN MATRIX:

The selected design matrix shown in the table was the central composite rotatable factorial design consisting 30 set of experiments. All variables at the intermediate (0) level constitute the center point while the combination of each variable at

either lower value (-2) or higher value (+2) with the other variables of the intermediate level compose the star points. Thus 30 experimental runs of design matrix were developed.

Table 4: Experimental Design Matrix and its actual values.

S.No	Coded Value				Actual Value			
	Laser Power (W)	Travel Speed (mm/min)	Defocusing Distance (mm)	Powder Feed Rate (g/min)	Laser Power (W)	Travel Speed (mm/min)	Defocusing Distance (mm)	Powder Feed Rate (g/min)
1	-1	-1	-1	-1	2400	500	18	8
2	1	-1	-1	-1	2800	500	18	8
3	-1	1	-1	-1	2400	700	18	8
4	1	1	-1	-1	2800	700	18	8
5	-1	-1	1	-1	2400	500	22	8
6	1	-1	1	-1	2800	500	22	8
7	-1	1	1	-1	2400	700	22	8
8	1	1	1	-1	2800	700	22	8
9	-1	-1	-1	1	2400	500	18	16
10	1	-1	-1	1	2800	500	18	16
11	-1	1	-1	1	2400	700	18	16
12	1	1	-1	1	2800	700	18	16
13	-1	-1	1	1	2400	500	22	16
14	1	-1	1	1	2800	500	22	16
15	-1	1	1	1	2400	700	22	16
16	1	1	1	1	2800	700	22	16
17	-2	0	0	0	2200	600	20	12
18	2	0	0	0	3000	600	20	12
19	0	-2	0	0	2600	400	20	12
20	0	2	0	0	2600	800	20	12
21	0	0	-2	0	2600	600	16	12
22	0	0	2	0	2600	600	24	12
23	0	0	0	-2	2600	600	20	4
24	0	0	0	2	2600	600	20	20
25	0	0	0	0	2600	600	20	12
26	0	0	0	0	2600	600	20	12
27	0	0	0	0	2600	600	20	12
28	0	0	0	0	2600	600	20	12
29	0	0	0	0	2600	600	20	12
30	0	0	0	0	2600	600	20	12

2.3 EVALUATING THE HARDNESS OF LASER HARD FACING SURFACES:

The laser hardfacing is carried out on AISI 304 stainless steel by using CO₂ laser with a maximum capacity of 4000W according to the design matrix at random order. The average deposited thickness was about 0.8–1.6 mm on the stainless steel. After hardfacing the deposit was cut into small samples for the SEM and hardness study. The preparation of the specimens is done by using Electrical Discharge Machining (EDM). A Vickers microhardness testing machine (Make: SHIMADZU, Japan; Model: HMV - 2T) was employed for measuring the hardness across the cross section of the deposit with a load of 0.5 kg and dwell time of 15 s. The laser hardfaced specimens were cut for evaluating the micro hardness and the subsequent values are noted. The same values are used for deriving the empirical relationship.



Figure1: Laser Hardfaced Samples.

III. DEVELOPING AN EMPIRICAL RELATIONSHIP

Hardness of Laser hardfaced surface is a function of the Laser parameters like as Laser power (P), Travel speed (T), Defocusing distance (D), powder feed rate (F), and it can be expressed as

$$\text{Hardness of deposit} = f(P, T, D, F)$$

The second-order polynomial equation used to predict the response surface Y is given by

$$Y = b_0 + \sum b_i x_i + \sum b_{ii} x_i^2 + \sum b_{ij} x_i x_j$$

And for four factor, the selected polynomial could be expressed equally

$$\text{Hardness} = [b_0 + b_1(P) + b_2(T) + b_3(D) + b_4(F) + b_{12}(PT) + b_{13}(PD) + b_{14}(PF) + b_{23}(TD) + b_{24}(TF) + b_{34}(DF) + b_{11}(P^2) + b_{22}(T^2) + b_{33}(D^2) + b_{44}(F^2)]$$

where, b_0 is the average of response and $b_1, b_2, b_3, \dots, b_4$ are regression co-efficient that depends on respective linear, interactions and square terms of factors. The value of co-efficient was calculated using Design Expert software at 95% confidence level. The significance of the each co-efficient was calculated from t-test and p values. The value of “Probe> F” is less than 0.05, indicates that model terms are significant. In this case P, T, D, F, PT, PD, PF, TD, TF, DF, P^2 , T^2 , D^2 , and F^2 are the significant terms. The final empirical relationship was built using only these co-efficient and the established final empirical relationship of laser hardfaced deposit of Stellite-6 alloy is given below.

Table 5: Anova Test Results:

Source	Sum of Squares (SS)	Degree of Freedom	Mean Square	F-value	p-Value (Prob > F)	Significant or Not
Model	94677.62	14	6762.69	233.15	< 0.0001	Significant
P	2926.04	1	2926.04	100.88	< 0.0001	
T	3577.04	1	3577.04	123.32	< 0.0001	
D	5310.37	1	5310.37	183.08	< 0.0001	
F	7668.37	1	7668.37	264.38	< 0.0001	
PT	430.56	1	430.56	14.84	0.0016	
PD	232.56	1	232.56	8.02	0.0126	
PF	280.56	1	280.56	9.67	0.0072	
TD	264.06	1	264.06	9.1	0.0087	
TF	175.56	1	175.56	6.05	0.0265	
DF	1785.06	1	1785.06	61.54	< 0.0001	

P ²	34061.57	1	34061.57	1174.31	< 0.0001	Not Significant
T ²	25289.36	1	25289.36	871.88	< 0.0001	
D ²	1025.5	1	1025.5	35.36	< 0.0001	
F ²	32155.86	1	32155.86	1108.61	< 0.0001	
Residual	435.08	15	29.01			
Lack of Fit	325.75	10	32.57	1.49	0.3455	
Pure Error	109.33	5	21.87	Mean	437.90	
Cor. Total	95112.7	29		C.V. %	1.23	
Std. Dev.	5.39			PRESS	2033.76	
R-Squared	0.9954			Pred. R-Squared	0.9786	
Adj. R-Squared	0.9912			Adeq. Precision	47.233	

$$\begin{aligned} \text{Hardness} = & [-8251.79 + 4.73(P) + 2.78(T) + 97.02(D) + 100.81(F) + 2.5937 \text{ E-}004(PT) - 9.5312 \text{ E-}003(PD) \\ & - 5.23437 \text{ E-}003(PF) + 0.0203(TD) - 8.2812 \text{ E-}003(TF) - 1.32(DF) - 8.8099 \text{ E-}004(P^2) - \\ & 3.0364 \text{ E-}003(T^2) - 1.52(D^2) - 2.13(F^2)] \text{HV} \end{aligned}$$

The equation in terms of actual factor values can be used to make predictions about the response for given levels of each factor value. In this for each factor the levels should be indicated in the original units. To determine the relative impact of each factor this equation should not be used because the coefficients are scaled to billet the units of each factor and the intercept is not at the center of the design space. The adequacy of the above relation is tested by analysis of variance ANOVA. The ANOVA test results are given in Table 5. at the desired confidence level of 95%. The relationship may be considered to be adequate, if the calculated value of the F_{ratio} of the developed relationship does not exceed the tabulated value of F_{ratio} for an anticipated level of confidence and the model is found to be adequate. The Fisher's F-test with a very low probability value demonstrates a very high significance of the regression model. The goodness fit of the model is determination by the co-efficient (R^2). The coefficient of determination was calculated to be 0.99 in response which implies that 99% of the experimental values confirm the compatibility with data as predicted by the model. The value of R^2 should always lies between 0 and 1. Model is considered to be statistically good when the R^2 value should be close to 1.0. Then adjusted R^2 value reconstructs the expression with the significant terms. The value of adjusted $R^2 = 0.9912$ is also high which indicates the model is highly significance. The predicted R^2 value is 0.9786 which means that the model could explain 97.8% of the variability in prediction. This is a reasonable agreement with the adj. R^2 of 0.9912. The coefficient of variation is as low as 1.23, which specifies the deviation between predicted and experimental values are low. Adequate measures of the Signal to noise ratio, a ratio greater than 4 is desirable. During this investigation, the ratio is 47.23, which indicates the signal derived is adequate. This model can be used to navigate the design space. The correlation graph shows the predicted and actual hardness of laser hardfaced deposit, which could indicate the deviation between the actual and predicted hardness is low.

3.1 PREDICTED VALUES AND ACTUAL VALUES:

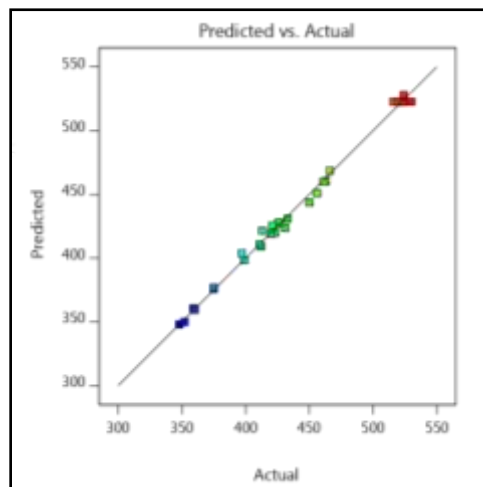


Figure2: Correlation Graph.

IV. OPTIMIZING THE LASER PARAMETERS

In general Response Surface Methodology is known as RSM an anthology of statistical analysis and mathematical methods that are helpful in optimizing process parameters. Response Surface methodology is an assortment technique useful for modeling and optimizing and analyzing the experiments in which a response variable is influenced by several independent variables. RSM is applied to fit the acquired model to the desired model when random factors are present and it may fit linear or quadratic models to designate the response in terms of the independent variables and then search for the optimal settings for the independent variables by performing an optimization step. It explores the interactions between several independent variables and one or more response variables. The response variable can be graphically perceived as a function of the process variables and this graphical perspective of the problem has led to the term Response Surface Methodology. The RSM was built to check the accuracy of model parts which is used to build the time as function of the process variables and other parameters. Central composite designs (CCD) are appropriate for calibrating the full quadratic models described in Response Surface. There are three types of CCD, namely, circumscribed, inscribed and faced. Each design consists of a factorial design (the corners of a cube) together with center and star points that allow estimation of second order effects. For a full quadratic model with n factors, CCD have enough design points to estimate the $(n+2)(n+1)/2$ coefficient in a full quadratic model with n factors. The type of CCD used (the position of the factorial and star points) is determined by the number of factors and by the desired properties of the design. A design is rotatable if the prediction variance depends only on the distance of the design point from the center of the design.

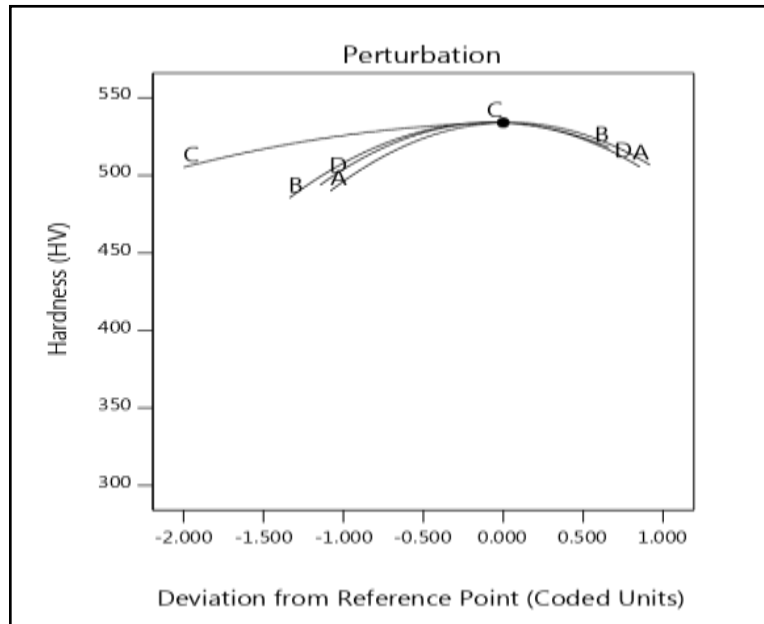


Figure 3: Perturbation Graph.

In Figure:3 perturbation plot for the response of hardness of the hardfaced layer are Illustrated. When each Laser Hardfacing parameter transfers from the reference point, with all other parameters held constant as the orientation value. This plot offers an outline view of the response and displays the transformation of hardness. The design of experiment, sets the reference point by default which is located in the middle of the design space. From perturbation graph and the response surface graphs, it can be observed that the hardness multiplies with the increasing Powder Feed Rate and defocusing distance to a certain level and then it starts decreases. It may be validated due to the inadequate energy or low-slung heat input causes the escaping of powders and partially melted partials existing in the hardfaced surface. Hardness drops with increasing laser power and travel speed. It may be assumed that the high heat input will turn up the depth of penetration and dilution of the deposits. Contour plot shows a vital role in the elucidation of the response surface. It is vibrant from that when the hardness increases with increasing Powder Feed Rate, defocusing distance and hardness decrease with increasing laser power.

Figure 4:(A-F) Response Surface Graphs and Contour Plots.

Figure 4A: Interaction effect of laser power and travel speed.

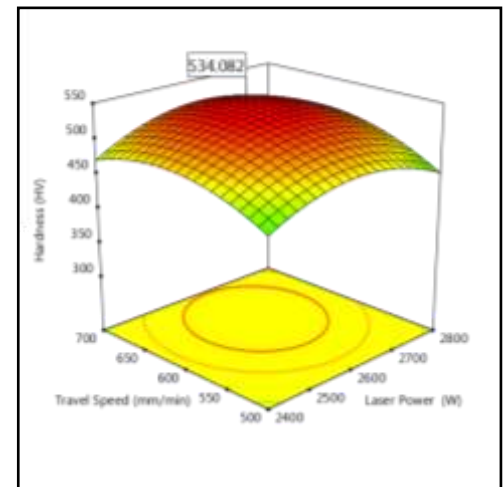
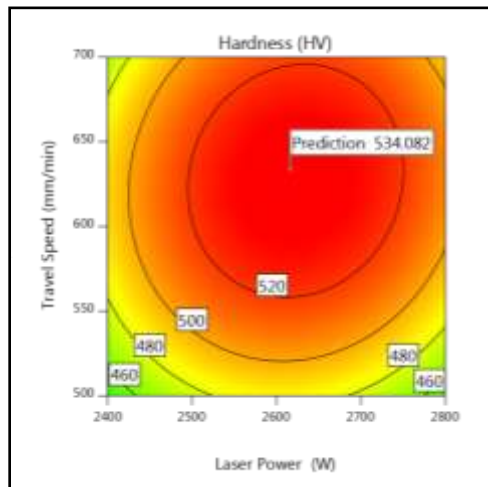


Figure 4B: Interaction effect of laser power and defocusing distance.

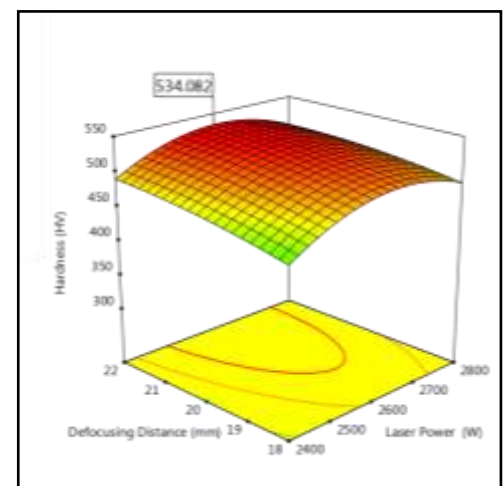
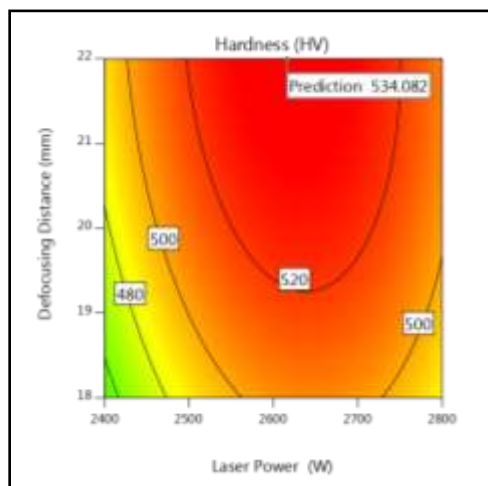


Figure 4C: Interaction effect of laser power and powder feed rate.

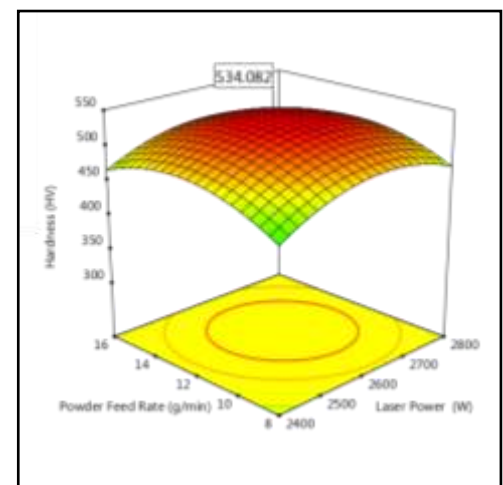
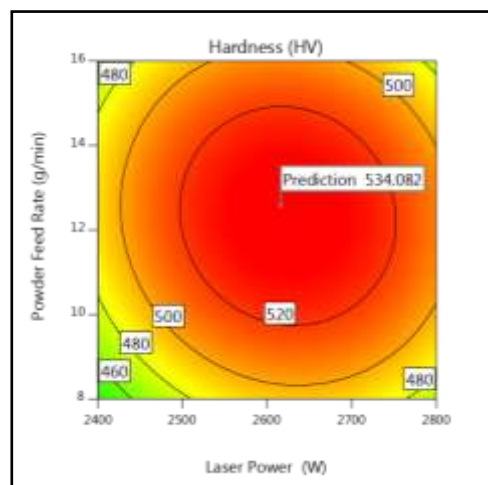


Figure 4D: Interaction effect of travel speed and defocusing distance.

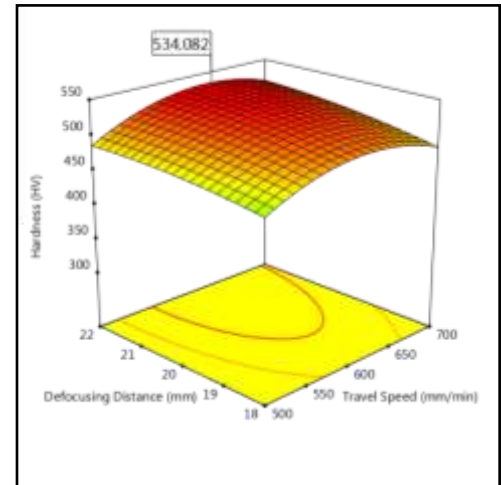
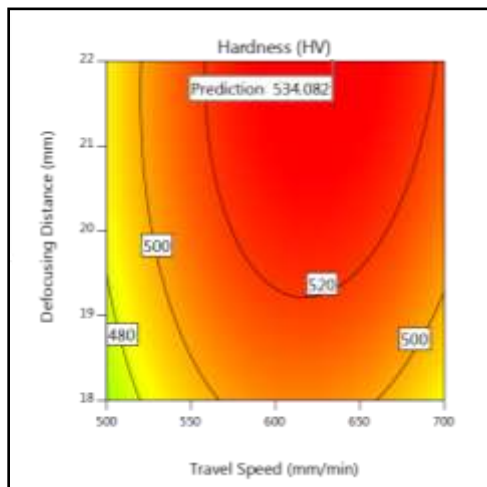


Figure 4E: Interaction effect of travel speed and powder feed rate.

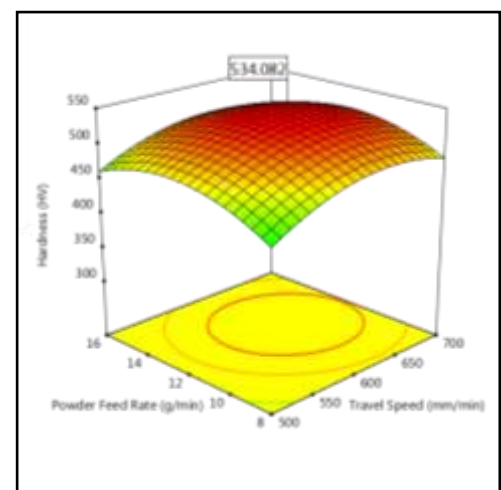
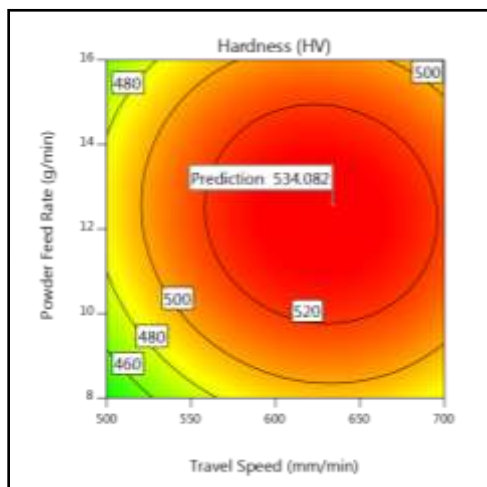


Figure 4F: Interaction effect of powder feed rate and defocusing distance.

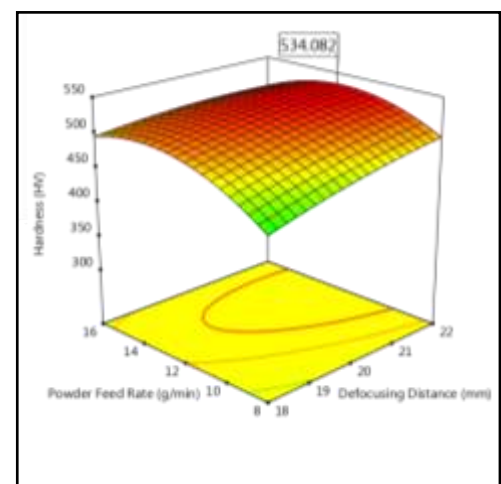
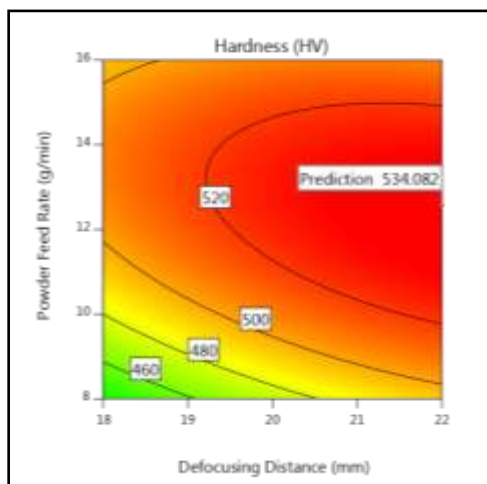


Figure 4 (A–F) shows that surface and contour plots for each process parameters. It is clear that the hardness increases and decreases with an increase of process parameters. Hardness mainly depends on dilution and microstructure. Laser power is predominantly used for melting the powder and excess heat melts the substrate. Keep on increasing the laser power high volume of substrate material melts which results in the proliferation on dilution. The hardness variation in laser hardfaced sample could be affected by the dilution. As the result of higher dilution the value of hardness will decrease and hence the dilution should be kept minimum. While increasing the laser power the dilution turns up hence the value of the hardness will be decreased. When there is an increase in powder feed rate there might be a decrease in dilution which results to the increase in the hardness value. This may be happened because the major amount of heat from the laser source is utilized for melting the powder and a very small amount of heat melts the substrate material. While increasing the Transfer speed, the powder density per square area becomes less so dilution rate is little bit increased and leads to the increase in hardness. when the defocusing distance increases there might be the reduction of power density per unit area and dilution whereas hardness multiplies to certain limit. By analyzing the response surface and contour plots as shown in Figure 4 (A–F), the maximum achievable hardness value is found to be 534.082 HV. The corresponding parameters exist maximum hardness value produced by 2616 W of Laser power, 633 mm/min of travel speed, 22 mm of defocusing distance and 12.5 g/min of Powder Feed Rate at the hill of response surface plot and corresponding domain in the contour plot. The optimized Value is tabulated in Table :6.

Table 6: Optimized Laser Hardfacing Parameters.

S. No	Important Laser Parameters	Optimized Value
1	Laser Power	2616 (W)
2	Travel Speed	633(mm/min)
3	Defocusing Distance	22(mm)
4	Powder Feed Rate	12.5(g/min)

V. CONCLUSIONS

1. An empirical relationship was developed to predict the hardness of cobalt-based(stellite-6) hardfaced surface produced on 304 Austenitic Stainless-Steel substrate with 95% confidence level by incorporating important Laser Hardfacing parameters.
2. The maximum achievable optimized hardness value is found to be 534.082 (HV). The corresponding parameters exist maximum hardness value produced by 2616 (W) of Laser power, 633 (mm/min) of travel speed, 22 (mm) of defocusing distance and 12.5 (g/min) of Powder Feed Rate.
3. The Powder Feed Rate is the major influencing factor to predict the hardness, among the other hardfacing parameters like as Laser power, Travel speed and Defocusing distance.

REFERENCES

- [1] M. K. Alam, N. Nazemi, R. J. Urbanic, S. Saqib, and A. Edrisy, "Investigating Process Parameters and Microhardness Predictive Modeling Approaches for Single Bead 420 Stainless Steel Laser Cladding," August, 2016.
- [2] P. Balu, P. Leggett, S. Hamid, and R. Kovacevic, "Multi-response optimization of laser-based powder deposition of multi-track single layer hastelloy C-276," Mater. Manuf. Process., vol. 28, no. 2, pp. 173–182, 2013.
- [3] K. Y. Benyounis and A. G. Olabi, "Optimization of different welding processes using statistical and numerical approaches - A reference guide," Adv. Eng. Softw., vol. 39, no. 6, pp. 483–496, 2008.
- [4] Frenk and W. Kurz, "High speed laser cladding: solidification conditions and microstructure of a cobalt-based alloy," Mater. Sci. Eng. A, vol. 173, no. 1–2, pp. 339–342, 1993.
- [5] S. Guo, Z. Chen, D. Cai, Q. Zhang, V. Kovalevko, and J. Yao, "Prediction of simulating and experiments for cobalt-based alloy laser cladding by HPDL," Phys. Procedia, vol. 50, October 2012, pp. 375–382, 2013.
- [6] C. J. Heuvelman, "Surface Treatment Techniques by Laser Beam Machining," CIRP Ann. - Manuf. Technol., vol. 41, no. 2, pp. 657–666, 1992.
- [7] S. Liu and R. Kovacevic, "Statistical analysis and optimization of processing parameters in high-power direct diode laser cladding," Int. J. Adv. Manuf. Technol., vol. 74, no. 5–8, pp. 867–878, 2014.
- [8] F. Madadi, F. Ashrafzadeh, and M. Shamanian, "Optimization of pulsed TIG cladding process of stellite alloy on carbon steel using RSM," J. Alloys Compd., vol. 510, no. 1, pp. 71–77, 2011.

- [9] B. R. Moharana, S. K. Sahu, S. K. Sahoo, and R. Bathe, "Experimental investigation on mechanical and microstructural properties of AISI 304 to Cu joints by CO₂ laser," *Eng. Sci. Technol. an Int. J.*, vol. 19, no. 2, pp. 684–690, 2016.
- [10] K. S. H. Prasad, C. S. Rao, and D. N. Rao, "Application of Design of Experiments to Plasma Arc Welding Process: A Review," *J. Brazilian Soc. Mech. Sci. Eng.*, vol. 34, no. 1, pp. 75–81, 2012.
- [11] S. Saqiba, R. J. Urbanica, and K. Aggarwal, "Analysis of laser cladding bead morphology for developing additive manufacturing travel paths," *Procedia CIRP*, vol. 17, pp. 824–829, 2014.
- [12] K. Siva, N. Murugan, and V. Raghupathy, "Modelling, analysis and optimisation of weld bead parameters of nickel based overlay deposited by plasma transferred arc surfacing," *Surf. Eng.*, vol. 1, 2009, pp. 174–182, 2009.
- [13] Tabernero, A. Calleja, A. Lamikiz, and L. N. López De Lacalle, "Optimal parameters for 5-axis Laser cladding," *Procedia Eng.*, vol. 63, pp. 45–52, 2013.
- [14] X. Wang, "Modeling and optimization of laser transmission joining process between PET and 316L stainless steel using response surface methodology," *Opt. Laser Technol.*, vol. 44, no. 3, pp. 656–663, 2012.
- [15] P. Wen, Z. Feng, and S. Zheng, "Formation quality optimization of laser hot wire cladding for repairing martensite precipitation hardening stainless steel," *Opt. Laser Technol.*, vol. 65, January 2015, pp. 180–188, 2015.
- [16] S. Y. Wen, Y. C. Shin, J. Y. Murthy, and P. E. Sojka, "Modeling of coaxial powder flow for the laser direct deposition process," *Int. J. Heat Mass Transf.*, vol. 52, no. 25–26, pp. 5867–5877, 2009.